



Published in final edited form as:

Invest Ophthalmol Vis Sci. 2004 February ; 45(2): 635–640.

Inhibition of Choroidal Neovascularization in Rats by the Urokinase-Derived Peptide Å6

Hyoung J. Koh^{1,2}, Kenichiro Bessho¹, Lingyun Cheng¹, Dirk-Uwe Bartsch¹, Terence R. Jones³, Germain Bergeron-Lynn¹, and William R. Freeman¹

¹From the Joan and Irwin Jacobs Retina Center, Department of Ophthalmology, Shiley Eye Center, University of California, San Diego, California; the

²Department of Ophthalmology, Yonsei University College of Medicine, Seoul, Korea; and

³Ångstrom Pharmaceuticals, San Diego, California.

Abstract

Purpose—To evaluate the inhibitory effects of a urokinase-derived octapeptide Å6 on laser-induced choroidal neovascularization (CNV).

Methods—In the first arm of the study, subcutaneous injection of Å6 (200 mg/kg per day) into the right eyes in 20 rats and phosphate-buffered saline in 20 control rats was started 1 day before laser injury. Angiography was performed at week 2. To evaluate the dose response, a second arm of the study was performed in the left eyes. Half of the treatment group was treated with 400 mg/kg per day, and the remaining half continued to receive 200 mg/kg per day beginning on week 4. Laser injury was made at week 5 and angiography was performed at week 7. Angiographic evaluation, histopathologic evaluation including maximum CNV thickness and factor-VIII–stained endothelium counting were performed in the second arm of the study. Choroidal concentrations of Å6 were measured.

Results—In the first arm of the study, angiography showed a 40.8% reduction in CNV in the 200-mg/kg per day treatment group, compared with the control ($P = 0.0008$). In the second arm of the study, angiographic reduction in CNV was 37.9% in the 200-mg/kg per day group ($P = 0.0314$) and 70.0% in the 400-mg/kg per day group ($P = 0.0124$), compared with the control. CNV was significantly less in the 400-mg/kg per day group than in the 200-mg/kg per day group ($P = 0.0393$). Both CNV thickness and number of endothelial cells were reduced in a dose-dependent manner and significantly less than in the control ($P < 0.05$). Mean choroidal concentration of Å6 2 hours after injection was 0.72 μM in the 200-mg/kg per day (100 mg/kg every 12 hours) and 1.75 μM in the 400-mg/kg per day (200 mg/kg every 12 hours) treatment groups. Levels at 11 hours after injections were undetectable.

Conclusions—Å6 demonstrated antiangiogenic properties in a rat model of CNV and may be useful in the treatment of CNV.

Age-related macular degeneration, characterized by CNV, is the leading cause of irreversible vision loss in the United States.¹ Various treatments have been attempted, including laser

Corresponding author: William R. Freeman, Joan and Irwin Jacobs Retina Center, Department of Ophthalmology, Shiley Eye Center, University of California, San Diego, 9415 Campus Point Drive, La Jolla, CA; freeman@eyecenter.ucsd.edu.

Presented at the annual meeting of the Association for Research in Vision and Ophthalmology, Fort Lauderdale, Florida, May 2003.

Disclosure: **H.J. Koh**, None; **K. Bessho**, None; **L. Cheng**, None; **D.-U. Bartsch**, None; **T.R. Jones**, Ångstrom Pharmaceuticals (F, E, P, R); **G. Bergeron-Lynn**, None; **W.R. Freeman**, Ångstrom Pharmaceuticals (C)

Supported in part by Research to Prevent Blindness and unrestricted donations from the University of California, San Diego.

photocoagulation, photodynamic therapy, and macular translocation. However, the visual prognosis is still poor in most patients with the disease.²⁻⁶

CNV is a result of pathologic angiogenesis. Angiogenesis is an invasion process that requires proteolysis of the extracellular matrix and proliferation and migration of endothelial cells, with simultaneous synthesis of new matrix components.⁷ Antiangiogenesis therapies have thus far focused on inhibitors of vascular endothelial growth factor (VEGF)^{1,8} and proteolytic enzymes such as matrix metalloproteinases (MMPs).⁹⁻¹⁴ As the pathogenesis of angiogenesis becomes better understood, new drug targets are emerging.

Urokinase plasminogen activator (uPA), together with its receptor uPAR, is a pleiotropically acting system that has been studied intensively over the past several decades, mainly in the field of cancer, where it has become deeply implicated in several pathologic aspects of this disease. The binding of uPA to uPAR triggers twin cascades of events, the first of which is destruction of the extracellular matrix (ECM). The second is intracellular signaling to program gene expression leading to cell migration, cell invasion, metastasis, and angiogenesis.¹⁵⁻¹⁹

Only in more recent years has the involvement of uPA/uPAR been demonstrated in ocular disease. High levels of urokinase have been observed in neovascular membranes surgically removed from patients with proliferative diabetic retinopathy.²⁰ Recently, it was shown that VEGF-induced sustained paracellular permeability in cultured retinal microvascular endothelial cells is mediated by uPA/uPAR.²¹ Overexpression of the uPA/uPAR system has been shown during retinal neovascularization,²² in surgically excised CNV,⁷ and in laser-induced CNV.⁷ uPA/uPAR has been found to play a key role in the migration of human retinal pigment epithelial cells through ECM-like layers in vitro.²³ Enhanced levels of uPAR have been found in surgically excised CNV and proliferative vitreoretinopathy membranes.²³ Oxygen-induced retinal neovascularization is reduced in homozygous uPAR^{-/-} mice.²² Homozygous uPA^{-/-} mice also demonstrate decreased CNV development in a laser-induced CNV model.⁷

Angiogenesis is a multistage process. It starts with a growth factor binding to dormant endothelial cells to cause their rapid proliferation. In cancer, VEGF, insulin-like growth factor (IGF), FGF, IL-8, hepatocyte growth factor (HGF), TGF- α , and TGF- β have been identified in this role, and in surgically excised human CNV tissue, VEGF,^{24,25} FGF,²⁶ and TGF- β .²⁶ A later stage of angiogenesis is the controlled migration of this expanded endothelial cell population to form a new microcapillary, in which the uPA/uPAR system probably plays the key role.²⁷ Thus, one can view the uPA/uPAR system as the final common pathway through which angiogenesis is completed, no matter what growth factor started it. Indeed, of those three growth factors identified in human CNV, TGF- β upregulates mRNA for uPA in human umbilical vein endothelial cells, a good substitute for human choroidal endothelial cells.²⁸ VEGF induces uPA/uPAR activity in bovine retinal endothelial cells,²¹ and FGF is well known to upregulate uPA/uPAR in several types of endothelial cell.²⁹⁻³² Therefore, the uPA/uPAR system could be a therapeutic target for antiangiogenic therapy for CNV.

The octapeptide $\text{\AA}6$ is derived from the non-receptor-binding region of uPA.³³ It is not antiproliferative.^{34,35} The ability of $\text{\AA}6$ to inhibit endothelial cell migration in vitro,^{33,34} angiogenesis,³³⁻³⁵ tumor cell invasion in vitro,^{33,35,36} tumor growth,³³⁻³⁶ and tumor metastasis^{33,35,36} in models of glioblastoma,³⁴ breast cancer,^{33,35} and prostate cancer³⁶ have all been demonstrated. $\text{\AA}6$ also inhibits hypoxia-induced retinal neovascularization.²² The purpose of this study was to evaluate the inhibitory effect of $\text{\AA}6$ on laser-induced CNV in the rat.

Materials and Methods

Administration of Å6 Peptide and Control

Forty Brown Norway rats weighing between 170 and 300 g were used in the study, in accordance with the guidelines of the University of California San Diego, Office of Veterinary Affairs, and the ARVO Statement for the Use of Animals in Ophthalmic and Vision Research.

We chose two sets of study parameters, using all right eyes in the first arm of the study and all left eyes for the second arm of the study (Fig. 1), after it was ascertained that the visual response and behavior of the animals was not altered with bilateral laser treatment.

The purpose of the first arm of the study was to evaluate the effect of our initial dose (200 mg/kg per day, i.e., 100 mg/kg every 12 hours). This dose was based on doses that have been shown to inhibit tumor growth in glioblastoma³⁴ and breast cancer models.^{33,35} In the second arm of the study, we doubled the dose (400 mg/kg per day, i.e., 200 mg/kg every 12 hours) starting 1 week before laser-induced CNV in 10 animals, to determine the effect of a higher dose given 1 week before laser treatment, which would potentially allow a steady state intraocular drug level to be achieved as occurs with certain other therapeutic agents^{37,38} and to determine whether the higher dose is more effective.

In the first arm of the study in right eyes, 40 animals were divided into treatment and control groups, each consisting of 20 animals. Å6, a capped peptide (Acetyl-Lys-Pro-Ser-Ser-Pro-Pro-Glu-Glu-NH₂; Ångstrom Pharmaceuticals, San Diego, CA) was injected twice daily subcutaneously (200 mg/kg per day), starting 1 day before the laser treatment and continuing to the end of the study. The control group received phosphate-buffered saline. Angiography was performed at week 2.

The second arm of the study in left eyes was undertaken to evaluate the dose–response relationship. Angiographic evaluation; histopathologic evaluation, including maximum CNV thickness; and factor-VIII–stained endothelium counting were performed in this arm. Half of the treatment group ($n = 10$) was treated with 400 mg/kg per day and the remaining half ($n = 10$) continued to receive 200 mg/kg per day, beginning on week 4. Laser injury was made at week 5, and angiography was performed at week 7.

Laser-Induced CNV

The rats were anesthetized for all procedures with intraperitoneal ketamine (21 mg/kg) and xylazine (5.25 mg/kg). The pupils were dilated with 0.5% cyclopentolate, 1% tropicamide, and 0.25% phenylephrine. The fundus was visualized with a 5.4-mm rat fundus laser lens (Ocular Instruments, Bellevue, WA) with 2.5% hydroxypropyl methyl-cellulose solution. A diode laser (Oculight SLx; Iridex Co., Mountain View, CA) with an 810-nm wave length was used. Laser parameters were 75- μ m spot size, 0.05-second exposure, and 250-mW power. A pattern of eight lesions was concentrically placed around the optic nerve. Formation of a bubble indicated rupture of Bruch's membrane.

In the second arm of the study in left eyes, each laser injury was made more peripherally from the optic nerve to avoid confluence of CNV lesions. One surgeon (HJK) performed all procedures.

Fluorescein and Indocyanine Green Angiography

Both fluorescein and indocyanine green (ICG) angiography were performed on weeks 2 and 7 with a confocal scanning laser ophthalmoscope (Heidelberg Retinal Angiograph; Heidelberg Engineering, Carlsbad, CA). Two milligrams of sodium fluorescein and 0.2 milligrams of ICG

mixture in 0.15 mL were injected intravenously followed by a bolus saline flush. Both fluorescein and ICG angiography were performed to capture the early (<2 minutes) and late (10 minutes) fluorescein phases and the late ICG phase (50 minutes) after injection.

CNV formation was determined with fluorescein angiograms taken 2 weeks after laser injury. Each laser lesion was classified as “leaky” or “non- or minimally leaky”^{39–41} by consensus of two observers (HJK, WRF). Leaky vessels were regarded as angiographically defined CNV. In cases of large subretinal hemorrhage that interfered with interpretation, the lesion was excluded. In some difficult-to-interpret cases, we also used the ICG angiographic finding.⁴¹ Angiograms were read in a masked manner. Consensus was reached on all angiograms.

Histopathologic Study

In the second arm of the study, morphometric measurement of CNV thickness, and immunostaining studies were performed in left eyes. Treated CNV lesions were compared with the contemporaneous control lesions, which had been induced with the same pattern of laser injury.

After final angiography, the rats were killed and eyes were enucleated and fixed in 4% phosphate-buffered paraformaldehyde solution (pH 7.4). Globes were dissected through the optic nerve and were processed for routine paraffin-embedded sectioning. Six-micrometer serial sections were cut for hematoxylineosin staining or immunostaining.

For morphometric measurement of CNV thickness, five eyes were randomly selected from each of the groups: 400 or 200 mg/kg per day and the control group. In hematoxylineosin-stained sections, a spindle-shaped subretinal fibrovascular scar was obvious and could be distinguished from adjacent normal structure. The maximum vertical meridian passing through this spindle-shaped scar was measured as the thickness. All the sections of each lesion were measured, and the highest thickness was chosen for analysis and comparison. This measurement was made with an eyepiece reticule after calibration with a stage micrometer with 10- μ m divisions (Olympus, Tokyo, Japan).

For immunostaining studies, 10 CNV lesions in each of the three groups were selected. A rabbit polyclonal antibody against factor VIII (1:750, Dako, Carpinteria, CA) was used to identify vascular endothelium within CNV. Factor-VIII-stained endothelial cells in CNV were counted on the representative sections that were immediately adjacent to the thickest portion of CNV. Rat spleen was used as a positive control. Adjacent sections were incubated without primary antibody and served as the negative control.

Measurement of Choroidal Concentration of Å6 Peptide

Twelve right eyes were randomly selected and used for the measurement of choroidal concentrations of Å6 peptide at two time points after injection at the end of a 7-week course of twice-daily injection. For early concentration measurements, three eyes from both the 400-mg/kg per day (200 mg/kg every 12 hours) and 200-mg/kg per day (100 mg/kg every 12 hours) treatment groups were enucleated 2 hours after injection. For late measurements, three eyes of each group were enucleated 11 hours after injection (1 hour before the scheduled evening injection). Eyeballs were enucleated after death at each time point and kept on ice until deep freezing and dissecting. The globe was submerged in -40°C 2-methyl butane in a beaker sitting in a dry ice ethanol bath for 30 seconds. The frozen globe was cut into halves through the optic nerve and further dissected under a surgical microscope into the vitreous, retina, choroid, and ciliary body/iris. All instruments were thoroughly cleaned between each sample collection. The different tissues from the same eyes were separately stored in the preweighed and prelabeled glass vials. The vials were again weighed, and the tissue weight was calculated. The

vials were stored at -70°C until analyzed for $\text{\AA}6$ content, conducted at MicroConstants (San Diego, CA). The choroidal tissues were homogenized with 0.5 mL of HPLC-grade water and ultrafiltered (Centrifree; Millipore, Bedford, MA). The ultrafiltrate was analyzed for $\text{\AA}6$ by reversed-phase chromatography (XDB-Phenyl column; Agilent, Wilmington, DE). Detection was achieved with a tandem quadrupole mass spectrometer (Micromass, Beverly, MA). The assay had a calibration range of 5 to 1000 ng/mL.

Statistical Analysis

Mann-Whitney U tests were used to compare the incidence of angiographically defined CNV. For analysis of CNV thickness and endothelial counts, nonparametric tests followed by nonparametric Tukey type multiple comparisons were used. For all analyses, a computer (JMP software ver. 4.1; SAS Inc., Cary, NC) was used, with $P < 0.05$ considered to be statistically significant.

Results

There was no difference in gains in body weight and behavioral patterns between $\text{\AA}6$ -treated and control rats. Angiography and histology showed no observable ophthalmoscopic side effect.

Incidence of Angiographically Defined CNV

In the first arm of the study, the incidence of angiographically defined CNV was 70.9% in the control group and 42.0% in the 200-mg/kg per day treatment group (Figs. 2, 3), corresponding to a 40.8% reduction ($P = 0.0008$).

In the second arm of the study, at the 200-mg/kg per day dose, the incidence of CNV was 50.6% in the control group and 31.4% in the treatment group. This corresponded to a 37.9% reduction ($P = 0.0314$). At the 400-mg/kg per day dose, the incidence of CNV was 44.7% in the control, whereas that of treatment group was 13.4%, corresponding to a 70.0% reduction ($P = 0.0124$).

The incidence of CNV was significantly less in the 400- than in the 200-mg/kg per day treatment group ($P = 0.0393$).

Histopathology of CNV

The maximum thickness of the CNV lesions was $90.05 \pm 19.07 \mu\text{m}$ in the control group, whereas that in 200-mg/kg per day treatment group was $74.67 \pm 22.34 \mu\text{m}$, a 17% reduction, and that in the 400-mg/kg per day treatment group was $60.59 \pm 20.57 \mu\text{m}$, a 33% reduction (Fig. 4, $P < 0.05$). The number of factor-VIII-stained endothelial cells in CNV were 48.9 ± 12.1 in the control group; 31.0 ± 14.4 in the 200-mg/kg per day group, a 37% reduction; and 16.80 ± 5.76 , in the 400-mg/kg per day group, a 66% reduction (Fig. 5, $P < 0.05$). CNV thickness and number of endothelial cells correlated negatively in a dose-dependent manner ($P < 0.001$, Spearman rho correlation).

Choroidal Concentration of $\text{\AA}6$ Peptide

In the 400-mg/kg per day (200 mg/kg every 12 hours) group, choroidal levels 2 hours after subcutaneous injection ranged between 774.1 ng/g ($0.85 \mu\text{M}$) and 2058.5 ng/g ($2.26 \mu\text{M}$), with a mean of 1594.2 ng/g ($1.75 \mu\text{M}$). The calculation of micromolar values assumes a tissue density of 1 g/mL. In the 200-mg/kg per day (100 mg/kg every 12 hours) group, 2-hour choroidal levels ranged between 283.9 ($0.31 \mu\text{M}$) and 1241.8 ng/g ($1.36 \mu\text{M}$), with a mean of 655.7 ng/g ($0.72 \mu\text{M}$). Levels at 11 hours were undetectable in each dose group.

Discussion

We evaluated the inhibitory effect of Å6 on CNV in angiograms taken 2 weeks after laser injury, because laser-induced CNV is known to reach its peak on day 14.⁴⁰ For interpretation of angiography, we compared early (<2 minute) and late (10 minute) frames of fluorescein angiography for each laser lesion. ICG angiography was used to confirm the fluorescein angiogram in difficult cases.

Recent publications have shown overexpression of uPA/uPAR in surgically excised human CNV^{7,23} and in laser-induced CNV in mice.⁷ Although the laser-induced CNV model does not completely mimic naturally occurring CNV in age-related macular degeneration,⁴² nonetheless, it is an appropriate model to evaluate the inhibitory effect of the Å6 peptide, because the uPA/uPAR system is present in both conditions.

We used one consistent parameter for all laser lesions made with a diode laser. In the first arm of the study, some subretinal CNV lesions coalesced. We, therefore, put laser burns much more peripherally to make interpretation clearer in the second arm of the study. Thus, the incidences of CNV in the control group were different between the first and second arms of the study.

In the second arm of the study, the dose–response relationship was analyzed both by angiography and histopathology, using the maximum thickness of CNV and number of endothelial cells within CNV. Angiographic reduction of CNV was striking when we doubled the dose: a 70.0% reduction in the 400-mg/kg per day treatment group and a 37.9% reduction in the 200-mg/kg per day treatment group. Both the maximum thickness of CNV and the number of endothelial cells within CNV were also decreased in a dose-dependent manner.

ICG angiography and histopathology revealed that some laser burns that were close to each other coalesced, and radial and horizontal dimensions were difficult to define in those cases. Each lesion was also very difficult to separate from the others, to measure the area in those cases. Therefore, we measured the maximum thickness instead of the area of CNV. Both CNV thickness and number of endothelial cells in the lesion decreased in a dose-dependent manner, constituting direct evidence of the inhibitory effect of Å6 on CNV.

Daily intravenous administration of Å6 for 7 days in mice at doses up to 1500 mg/kg is known to incur no toxicity (Meschter CA [Comparative Biosciences Inc., Mountain View, CA], personal communication, June 2002). Thus, it was no surprise to observe that no adverse effect or weight loss occurred in our rats in the 400-mg/kg per day group (data not shown). Continuous infusion and twice-daily injection yielded identical activities in an antitumor study.³³ Therefore, we elected to perform twice-daily subcutaneous injections.

Studies have demonstrated that the IC₅₀ for rat and human breast cancer cell invasion is 5 to 25 µM of the peptide and the IC₅₀ for human dermal microvascular endothelial cell migration is 25 to 50 µM.³³ In our experiment, after 7 weeks of twice-daily treatments, a mean 2-hour postinjection choroidal concentration of 0.72 µM was obtained with the 200-mg/kg per day treatment (100 mg/kg every 12 hours), and 1.75 µM with 400-mg/kg per day (200 mg/kg every 12 hours) treatment. Extensive Good Laboratory Practice standard toxicokinetic studies of Å6 administered daily subcutaneously in rats showed that after a 100-mg/kg dose, the 2-hour plasma level was 24.5 µM on the 28th day, after 28 injections; the plasma half-life was 0.5 hour (Jones TR, Ångstrom Pharmaceuticals, Inc., unpublished). The injection schedule in this CNV study was every 12 hours, potentially complicating the comparison, but because the attendant plasma half-life of Å6 is so brief, it is reasonable to assume that washout is complete before the next injection is given. With this proviso, if we compare 2-hour levels after a 100-mg/kg subcutaneous dose, the concentration measured in the choroid is 0.72 µM and that measured in the plasma is 24.5 µM. Assuming that peak levels in these tissue compartments

occur synchronously, the choroidal concentration of Å6 is 3% of that in the plasma. If we take this penetration value of 3% and apply it to the peak plasma level (C_{max}) of approximately 207 μM , known to occur 20 minutes after a 100-mg/kg subcutaneous dose in rats (Jones TR, Ångstrom Pharmaceuticals, Inc., unpublished), a peak choroidal concentration of 6.2 μM was derived. Because the pharmacokinetic parameters of subcutaneously injected Å6 scale linearly with dose (Jones TR, Ångstrom Pharmaceuticals, Inc., unpublished), it is possible to project a peak choroidal level of 12.4 μM in the high-dose group in this study. This is at the lower end of the range of the in vitro IC_{50} referred to above. Given these extrapolations, and taking into consideration none of the intraocular pharmacokinetic behavior of Å6, we conclude that Å6 reached a therapeutic concentration only intermittently during our study. Å6 must have been at subtherapeutic concentrations for most of the 12-hour period between injections, because it was not detected in the choroid at 11 hours. Despite this, the peptide was still therapeutic. Thus, it is possible that even better efficacy in CNV can be obtained with higher and more sustained concentrations of Å6 in the choroid.

Many drugs have poor penetration into the eye. At steady state, after an oral dose of 750 mg of ciprofloxacin, patients had a vitreous level 17% of that in serum.⁴³ After an intravenous 2-g dose of cefepime, the peak vitreal level, 2.86 $\mu\text{g/mL}$, is 2% of the peak serum level, 140.55 $\mu\text{g/mL}$.⁴⁴ The intraocular concentration of SU 10944, a VEGF inhibitor, intravenously administered in the rat, was 6% of that in plasma (Patel N, et al. *IOVS* 2003;44:ARVO E-Abstract 2903). When given orally at 5 mg/kg, there is no penetration of cyclosporine into the aqueous humor in patients with no or mild intraocular inflammation, but in patients with severe panuveitis (Behçet's disease), aqueous humor and vitreous levels were 22% and 16%, respectively, of that in the blood.⁴⁵

In this study, we demonstrated the inhibitory effect of Å6 peptide on CNV in a rat model, both angiographically and histopathologically. One advantage of Å6's inhibition of the uPA/uPAR system is that this pathway is a common mechanism in angiogenesis induced by VEGF, FGF, and other chemokines, such as $\text{TGF-}\beta$.^{24–26} Immunocytochemical studies have shown that uPA is widely distributed in eyes in the retinal pigment epithelium, choroid, and both the anterior and posterior layers of the retina.⁴⁶ Among these tissues, retinal pigment epithelium is regarded as a possible source of the uPA/uPAR system,²³ although this remains unclear.

Å6, derived from human uPA, was biologically active, even though its sequence (KPSSPPEE) differs from the corresponding sequence in the rat (KPSSTVDQ).³³ For application to human age-related macular degeneration, we hypothesize that Å6 will more potently inhibit the human uPA/uPAR system, and the activity we observed in rats may underpredict that which we would find in the clinic. Further studies to characterize the ocular pharmacokinetics and effect on ocular tissues are under way. A local intraocular delivery system that would allow for higher and more sustained choroidal levels of Å6 should provide a more optimal method to treat CNV in humans, and this possibility is currently being explored.

References

1. Krzystolik MG, Afshari MA, Adamis AP, et al. Prevention of experimental choroidal neovascularization with intravitreal anti-vascular endothelial growth factor antibody fragment. *Arch Ophthalmol* 2002;120:338–346. [PubMed: 11879138]
2. Moisseiev J, Alhalel A, Masuri R, Treister G. The impact of the macula photocoagulation study results on the treatment of exudative age-related macular degeneration. *Arch Ophthalmol* 1995;113:185–189. [PubMed: 7532394]
3. Treatment of Age-Related Macular Degeneration with Photodynamic Therapy (TAP) Study Group. Photodynamic therapy of sub-foveal choroidal neovascularization in age-related macular degeneration with verteporfin: two-year results of 2 randomized clinical trials-TAP report 2. *Arch Ophthalmol* 2001;119:198–207. [PubMed: 11176980]

4. Sharma S, Brown GC, Brown MM, Hollands H, Shah GK. The cost-effectiveness of photodynamic therapy for fellow eyes with subfoveal choroidal neovascularization secondary to age-related macular degeneration. *Ophthalmology* 2001;108:2051–2059. [PubMed: 11713079]
5. Mandal N, Chisholm IH. Identifying the proportion of age related macular degeneration patients who would benefit from photodynamic therapy with verteporfin (visudyne). *Br J Ophthalmol* 2002;86:118–119. [PubMed: 11801521]
6. American Academy of Ophthalmology. Macular translocation. *Ophthalmology* 2000;107:1015–1018. [PubMed: 10811099]
7. Rakic JM, Lambert V, Munaut C, et al. Mice without uPA, tPA, or plasminogen genes are resistant to experimental choroidal neovascularization. *Invest Ophthalmol Vis Sci* 2003;44:1732–1739. [PubMed: 12657615]
8. The Eyetech Study Group. Preclinical and phase IA clinical evaluation of an anti-VEGF pegylated aptamer (EYE001) for the treatment of exudative age-related macular degeneration. *Retina* 2002;22:143–152. [PubMed: 11927845]
9. Kvanta A, Shen WY, Sarman S, Seregard S, Steen B, Rakoczy E. Matrix metalloproteinase (MMP) expression in experimental choroidal neovascularization. *Curr Eye Res* 2000;21:684–690. [PubMed: 11120556]
10. Takahashi T, Nakamura T, Hayashi A, et al. Inhibition of experimental choroidal neovascularization by overexpression of tissue inhibitor of metalloproteinases-3 in retinal pigment epithelial cells. *Am J Ophthalmol* 2000;130:774–781. [PubMed: 11124297]
11. Ozerdem U, Mach-Hofacre B, Cheng L, et al. The effect of prinomastat (AG3340), a potent inhibitor of matrix metalloproteinases, on a subacute model of proliferative vitreoretinopathy. *Curr Eye Res* 2000;20:447–453. [PubMed: 10980656]
12. Cheng L, Rivero ME, Garcia CR, et al. Evaluation of intraocular pharmacokinetics and toxicity of prinomastat (AG3340) in the rabbit. *J Ocul Pharmacol Ther* 2001;17:295–304. [PubMed: 11436949]
13. Garcia C, Bartsch DU, Rivero ME, et al. Efficacy of prinomastat (AG3340), a matrix metalloproteinase inhibitor, in treatment of retinal neovascularization. *Curr Eye Res* 2002;24:33–38. [PubMed: 12187492]
14. Ozerdem U, Mach-Hofacre B, Varki N, et al. The effect of prinomastat (AG3340), a synthetic inhibitor of matrix metalloproteinases, on uveal melanoma rabbit model. *Curr Eye Res* 2002;24:86–91. [PubMed: 12187478]
15. Dano K, Andreasen PA, Grondahl-Hansen J, Kristensen P, Nielsen LS, Skriver L. Plasminogen activators, tissue degradation, and cancer. *Adv Cancer Res* 1985;44:139–266. [PubMed: 2930999]
16. Andreasen PA, Kjoller L, Christensen L, Duffy MJ. The urokinase-type plasminogen activator system in cancer metastasis: a review. *Int J Cancer* 1997;72:1–22. [PubMed: 9212216]
17. Dear AE, Medcalf RL. The urokinase-type-plasminogen activator receptor (CD87) is a pleiotropic molecule. *Eur J Biochem* 1998;252:185–193. [PubMed: 9523687]
18. Sidenius N, Blasi F. The urokinase plasminogen activator system in cancer: recent advances and implications for prognosis and therapy. *Cancer Metastasis Rev* 2003;22:205–222. [PubMed: 12784997]
19. Schmitt M, Wilhelm OG, Reuning U, et al. The urokinase plasminogen activator system as a novel target for tumour therapy. *Fibrinolysis Proteolysis* 2000;14:114–132.
20. Das A, McGuire PG, Eriqat C, Ober RR, De Juan E, Williams G. Human diabetic neovascular membranes contain high levels of urokinase and metalloproteinase enzymes. *Invest Ophthalmol Vis Sci* 1999;40:809–813. [PubMed: 10067990]
21. Behzadian MA, Windsor LJ, Ghaly N, Liou G, Tsai NT, Caldwell RB. VEGF-induced paracellular permeability in cultured endothelial cells involves urokinase and its receptor. *FASEB J* 2003;17:752–754. [PubMed: 12594181]
22. McGuire PG, Jones TR, Talarico N, Warren E, Das A. The urokinase/urokinase receptor system in retinal neovascularization: inhibition by $\tilde{A}6$ suggests a new therapeutic target. *Invest Ophthalmol Vis Sci* 2003;44:2736–2742. [PubMed: 12766081]
23. Elnor SG, Elnor VM, Kindzelskii AL, et al. Human RPE cell lysis of extracellular matrix: functional urokinase plasminogen activator receptor (uPAR), collagenase and elastase. *Exp Eye Res* 2003;76:585–595. [PubMed: 12697422]

24. Kvanta A, Algvare PV, Berglin L, Seregard S. Subfoveal fibrovascular membranes in age-related macular degeneration express vascular endothelial growth factor. *Invest Ophthalmol Vis Sci* 1996;37:1929–1934. [PubMed: 8759365]
25. Lopez PF, Sippy BD, Lambert HM, Thach AB, Hinton DR. Trans-differentiated retinal pigment epithelial cells are immunoreactive for vascular endothelial growth factor in surgically excised age-related macular degeneration-related choroidal neovascular membranes. *Invest Ophthalmol Vis Sci* 1996;37:855–868. [PubMed: 8603870]
26. Amin R, Puklin JE, Frank RN. Growth factor localization in choroidal neovascular membranes of age-related macular degeneration. *Invest Ophthalmol Vis Sci* 1994;35:3178–3188. [PubMed: 7519180]
27. Kjoller L. The urokinase plasminogen activator receptor in the regulation of the actin cytoskeleton and cell motility. *Biol Chem* 2002;383:5–19. [PubMed: 11928822]
28. Hackett SF, Campochiaro PA. Modulation of plasminogen activator inhibitor-1 and urokinase in retinal pigmented endothelial cells. *Invest Ophthalmol Vis Sci* 1993;34:2055–2061. [PubMed: 8491554]
29. Montesano R, Vassalli J-D, Baird A, Guillemin R, Orci L. Basic fibroblast growth factor induces angiogenesis in vitro. *Proc Natl Acad Sci USA* 1986;83:7297–7301. [PubMed: 2429303]
30. Mignatti P, Mazziere R, Rifkin DB. Expression of the urokinase receptor in vascular endothelial cells is stimulated by basic fibroblast growth factor. *J Cell Biol* 1991;113:1193–1201. [PubMed: 1645739]
31. Pepper MS, Sappino AP, Stocklin R, Montesano R, Orci L, Vassalli JD. Upregulation of urokinase receptor expression on migrating endothelial cells. *J Cell Biol* 1993;122:673–684. [PubMed: 8393013]
32. Gualandris A, Presta M. Transcriptional and posttranslational regulation of urokinase-type plasminogen activator expression in endothelial cells by basic fibroblast growth factor. *J Cell Physiol* 1995;162:400–409. [PubMed: 7860647]
33. Guo Y, Higazi AA-R, Arakelian A, et al. A peptide derived from the nonreceptor binding region of urokinase plasminogen activator (uPA) inhibits tumor progression and angiogenesis and induces tumor cell death in vivo. *FASEB J* 2000;14:1400–1410. [PubMed: 10877833]
34. Mishima K, Mazar AP, Gown A, et al. A peptide derived from the non-receptor-binding region of urokinase plasminogen activator inhibits glioblastoma growth and angiogenesis in vivo in combination with cisplatin. *Proc Natl Acad Sci USA* 2000;97:8484–8489. [PubMed: 10890917]
35. Guo Y, Mazar AP, Lebrun J-J, Rabbani SA. An antiangiogenic urokinase-derived peptide combined with tamoxifen decreases tumor growth and metastasis in a syngeneic model of breast cancer. *Cancer Res* 2002;62:4678–4684. [PubMed: 12183425]
36. Boyd DD, Kim S-J, Wang H, Jones TR, Gallick GE. A urokinase-derived peptide (Å6) increases survival of mice bearing orthotopically grown prostate cancer and reduces lymph node metastasis. *Am J Pathol* 2003;162:619–626. [PubMed: 12547719]
37. Kuppermann BD, Quiceno JI, Flores-Aguilar M, et al. Intravitreal ganciclovir concentration after intravenous administration in AIDS patients with cytomegalovirus retinitis: implications for therapy. *J Infect Dis* 1993;168:1506–1509. [PubMed: 8245536]
38. Taskintuna I, Rahhal FM, Capparelli EV, Cundy KC, Freeman WR. Intravitreal and plasma cidofovir concentrations after intravitreal and intravenous administration in AIDS patients with cytomegalovirus retinitis. *J Ocul Pharmacol Ther* 1998;14:147–151. [PubMed: 9572540]
39. Hikichi T, Mori F, Takamiya A, et al. Inhibitory effect of losartan on laser-induced choroidal neovascularization in rats. *Am J Ophthalmol* 2001;132:587–589. [PubMed: 11589891]
40. Takehana Y, Kurokawa T, Kitamura T, et al. Suppression of laser-induced choroidal neovascularization by oral tranilast in the rat. *Invest Ophthalmol Vis Sci* 1999;40:459–466. [PubMed: 9950606]
41. Hikichi T, Mori F, Sasaki M, et al. Inhibitory effect of bucillamine on laser-induced choroidal neovascularization in rats. *Curr Eye Res* 2002;24:1–5. [PubMed: 12187488]
42. Yanagi Y, Tamaki Y, Obata R, et al. Subconjunctival administration of bucillamine suppresses choroidal neovascularization in rat. *Invest Ophthalmol Vis Sci* 2002;43:3495–3499. [PubMed: 12407161]

43. Morlet N, Graham GG, Gatus B, et al. Pharmacokinetics of ciprofloxacin in the human eye: a clinical study and population pharmacokinetic analysis. *Antimicrob Agents Chemother* 2000;44:1674–1679. [PubMed: 10817727]
44. Aras C, Ozdamar A, Ozturk R, Karacorlu M, Ozkan S. Intravitreal penetration of cefepime after systemic administration to humans. *Ophthalmologica* 2002;216:261–264. [PubMed: 12207129]
45. BenEzra D, Maftzir G, de Courten C, Timonen P. Ocular penetration of cyclosporin A. III: The human eye. *Br J Ophthalmol* 1990;74:350–352. [PubMed: 2378841]
46. Tripathi RC, Tripathi BJ, Park JK. Localization of urokinase-type plasminogen activator in human eyes: an immunocytochemical study. *Exp Eye Res* 1990;51:545–552. [PubMed: 2123459]

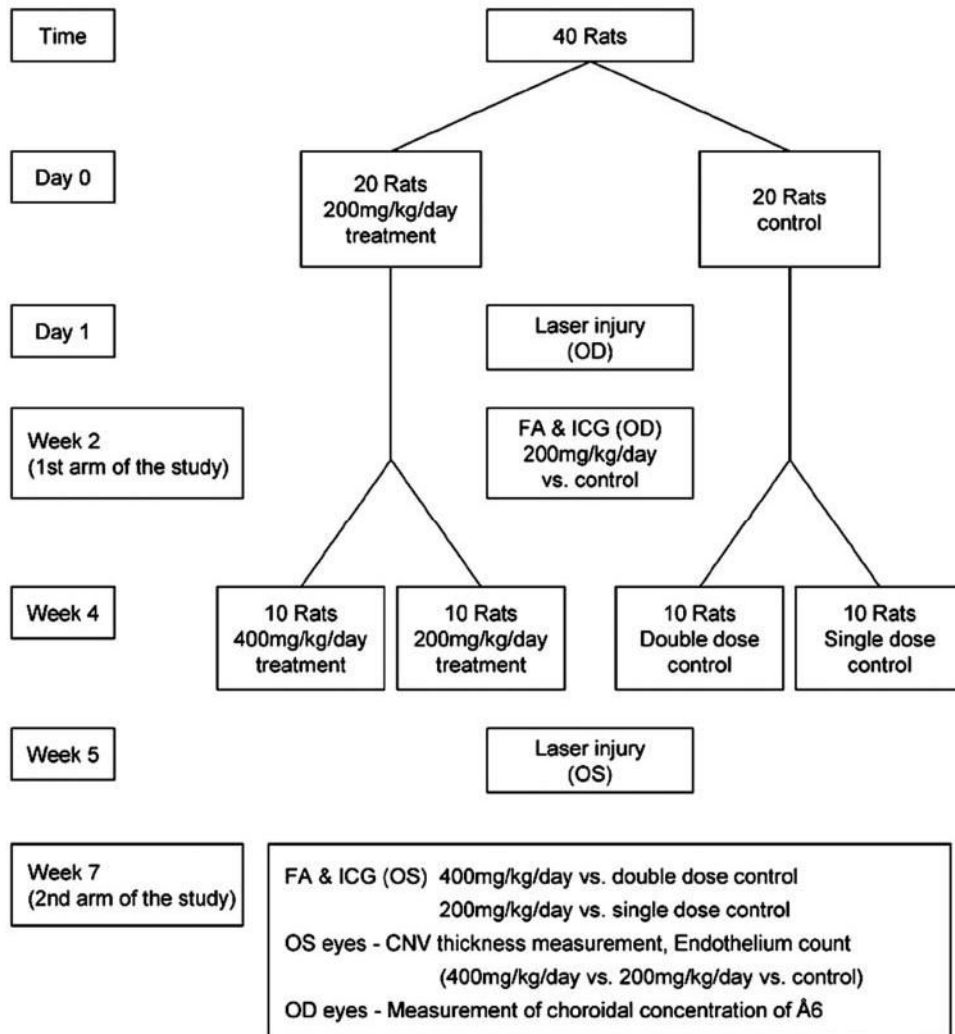


Figure 1.
Diagram of the study design.

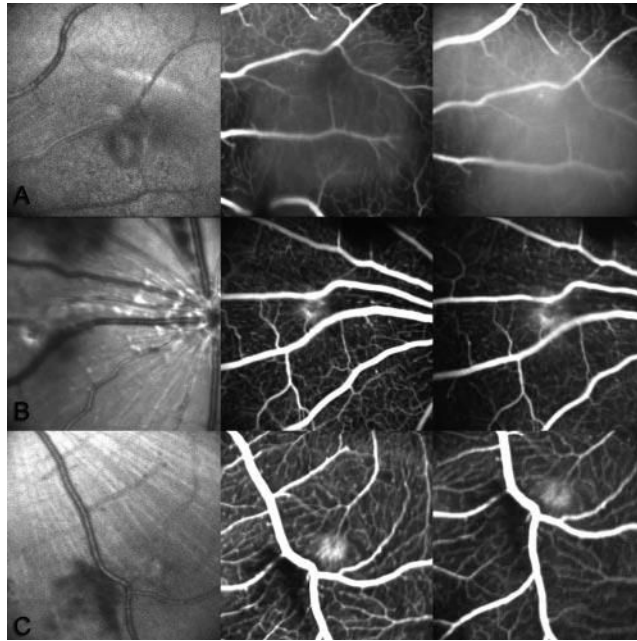


Figure 2. Representative red-free, early and late fluorescein angiography photos at 2 weeks after laser injury. (A) Control group and (B) 200- and (C) 400-mg/kg per day Å6-treated groups. There was intense leaking in laser-induced lesions in the control group, whereas there was minimal or no leaking in lesions in the Å6-treated group.

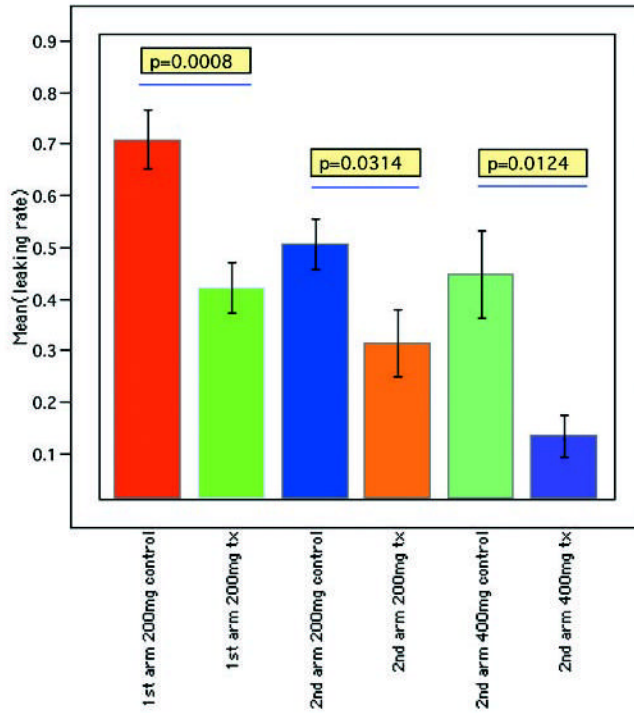


Figure 3.

Results of angiographic incidence of CNV in the control and Å6-treated groups. Data are the mean incidence of CNV \pm SEM. In both arms of the study, Å6-treated groups showed significantly less CNV than the control. In the second arm of the study, Å6-treated groups showed inhibition of CNV in a dose-dependent manner.

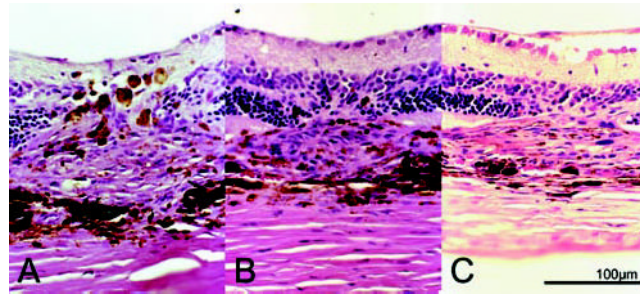


Figure 4. Hematoxylineosin stained light micrograph of CNV lesions 2 weeks after laser injury. Each photograph shows the center of CNV lesions in (A) the control group and (B) the 200- and (C) the 400-mg/kg per day Å6-treated groups.

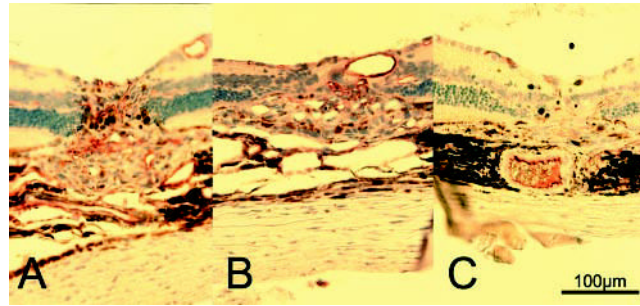


Figure 5. Typical endothelial cells immunostained with factor VIII in CNV 2 weeks after laser injury. (A) Control group and (B) 200- and (C) 400-mg/kg per day Å6-treated group. The number of immunoreactive vascular endothelial cells in CNV lesions was smaller in Å6-treated eyes.